Chinese Chemical Letters 36 (2025) 109968

Contents lists available at ScienceDirect

Chinese Chemical Letters

journal homepage: www.elsevier.com/locate/cclet

Chiral supramolecular catalysts of helical nanoribbon: More twist, higher enantioselectivity

Cong Gao, Zijian Zhu, Siwei Li, Zheng Xi*, Qingqing Sun*, Jie Han*, Rong Guo

School of Chemistry and Chemical Engineering, Yangzhou University, Yangzhou 225002, China

ARTICLE INFO

Article history:
Received 14 March 2024
Revised 16 April 2024
Accepted 5 May 2024
Available online 7 May 2024

Keywords:
Chiral supramolecular catalyst
Helical nanoribbon
Screw pitch
Enantioselectivity
Diels-Alder reaction

ABSTRACT

Rational tuning of chiral nanostructures of supramolecular assemblies as catalysts and investigating their chiral morphology-enantioselectivity dependence is rarely reported. Herein, we report a series of supramolecular *M*/*P*-helical nanoribbons (HNs) assembled from the chiral L/D-glutamate-based amphiphiles (L/D-GluC$_{16}$) and Cu(II) ions, with their helical screw pitches adjusted from 217 nm to 104 nm through the facile regulation of their water/organic solvent assembly environment. They were then used as ideal models to reveal the chiral morphology-enantioselectivity relationship by catalyzing the asymmetric Diels-Alder reaction. Better enantioselectivity was achieved with more twist morphology. Experimental evidences of stronger chiral transfer effect from the supramolecular HNs with more twist to the aza-chalcone as reactant were obtained to understand such dependence. Our study demonstrates a new perspective for designing supramolecular catalysts with higher enantioselectivity.

Developing an efficient catalyst with high enantioselectivity for organic asymmetric reactions is an overarching yet challenging goal for wide applications in the field of pharmaceutics, agricultural and food science, manufacturing industry and so on [1-7]. Compared with the small chiral molecular catalysts with limited stereoselective adjustability, the supramolecular catalysts based on chiral organic scaffolds have demonstrated greater promise, mainly due to their flexible tunability from both the chiral building blocks of organic units and chiral microenvironments of overall structures [8-12]. Understanding of the relationship between the chiral morphology and catalysis will advisably contribute to utilizing the stereochemical control and chiral amplification effect to maximize the enantioselectivity in asymmetric reactions [13]. Though some supramolecular structures such as helical bands [14,15], nanotubes [16,17] and nanofibers [18,19] formed by self-assembly of amphiphiles in solvents have been reported for capably catalyzing certain enantioselective reactions, the detailed study of the dependence between the chiral morphology control and enantioselective catalysis has rarely been achieved [20]. This dilemma is largely caused by lacking the efficient method to systematically accomplish the rational tuning of chiral morphology of the supramolecular catalysts.

Herein, we report a facile strategy to achieve the rational control of the chiral morphology of supramolecular helical nanoribbons (HNs) assembled from the L/D-glutamate-based amphiphiles (L/D-GluC$_{16}$) and Cu(II) ions. Specifically, the left or right-handedness (*M*/*P*) of the HNs was dependent on the chiral assembled units of L/D-GluC$_{16}$, respectively. More importantly, their helical screw pitch length can be easily adjusted through merely changing the kind of initial organic solvents they assembled in. By loading them with the same ratio of the Cu(II) ions as catalytic centers for asymmetrically catalyzing Diels-Alder (D-A) reaction, we demonstrate their enantioselectivity displays 4.5-fold enhancement as the screw pitch reduces from 217 nm to 104 nm, yet the unassembled L/D-GluC$_{16}$ amphiphiles alone show no enantioselectivity at all. Experimental evidences of stronger chiral transfer effect from the supramolecular HNs with more twist (smaller pitch length and larger tilt angle) to the aza-chalcone as reactant were obtained to help understand such chiral morphology-enantioselectivity dependence, which could provide guidance for designing chiral supramolecular catalysts with higher enantioselectivity.

To prepare the supramolecular *M*-HN–Cu(II), the pre-synthesized L-GluC$_{16}$ chiral amphiphiles (4×10^{-5} mol, characterized by ^{1}H and ^{13}C NMR spectra and mass spectrometry in Figs. S1 and S2 in Supporting information) were first dissolved in various organic solvent (1 mL), followed by the addition of water (9 mL) to initiate the self-assembly processes. After 15 min, *M*-HN were

* Corresponding authors.
E-mail addresses: xizheng@yzu.edu.cn (Z. Xi), sunqingqing@yzu.edu.cn (Q. Sun), hanjie@yzu.edu.cn (J. Han).

https://doi.org/10.1016/j.cclet.2024.109968
1001-8417/

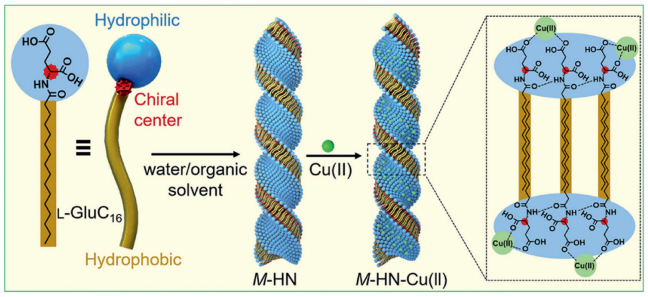

Scheme 1. Illustration of the self-assembly of L-GluC$_{16}$ and Cu(II) into supramolecular *M*-HN–Cu(II).

formed, with the following addition of 1 mol% of Cu(II) loaded onto the supramolecular HNs as the catalytic centers (Scheme 1 and details in Supporting information). The supramolecular *M*-HN–Cu(II) with different screw pitches were then just simply obtained from the self-assembly of the L-GluC$_{16}$ amphiphiles in the mixture of water and various organic solvents with fixed volume ratio. By defining the screw pitch l and tilt angle θ (illustrated in Fig. 1A), we can visually characterize and compare their different twist levels. Scanning electron microscope (SEM) images (Figs. 1B-F) exhibit the same left-handed morphology of one typical HN assembled in the water miscible mixture with acetone, methanol, ethanol, acetonitrile and tetrahydrofuran, respectively. Specifically, the *M*-HN–Cu(II) formed in the acetone/H_2O has a pitch of about 217 nm. However, when we changed acetone to other organic solvents while keeping the same ratio of organic solvent/water, the pitch of the *M*-HN–Cu(II) gradually reduced to 194 nm (methanol), 154 (ethanol), 121 nm (acetonitrile) and 104 nm (tetrahydrofuran). Atomic force microscopy (AFM) images with their corresponding height scan analyses demonstrate the five HNs all have the same assembly thickness of about 27 nm (Fig. S3 in Supporting information). Among the five samples, the HNs assembled from tetrahydrofuran (Fig. 1F) have the average shortest

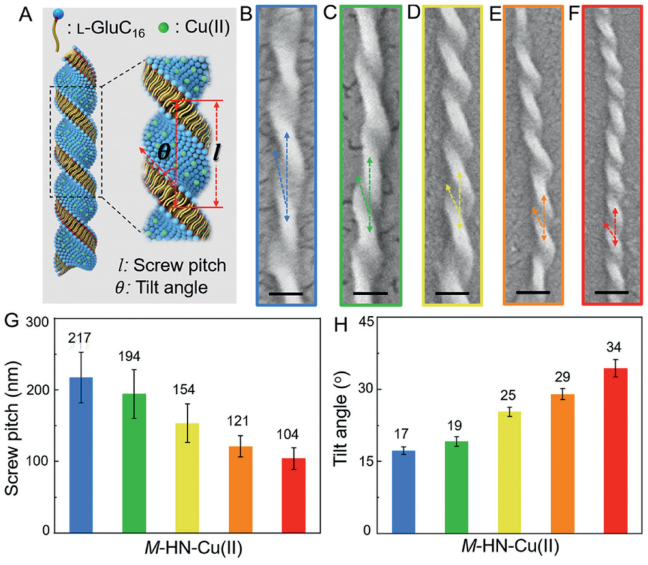

Fig. 1. (A) Schematic illustration of the *M*-HN–Cu(II) with the definition of screw pitch and tilt angle. SEM images of one typical *M*-HN–Cu(II) with different screw pitches and tilt angles assembled in water mixture with (B) acetone, (C) methanol, (D) ethanol, (E) acetonitrile and (F) tetrahydrofuran. Histograms of average (G) screw pitch length and (H) tilt angle degree for the *M*-HN–Cu(II) assembled in different water/organic mixture solvent. The bar colors correspond to the kind of water/organic mixtures they assembled in from B to F. Scale bars are 100 nm.

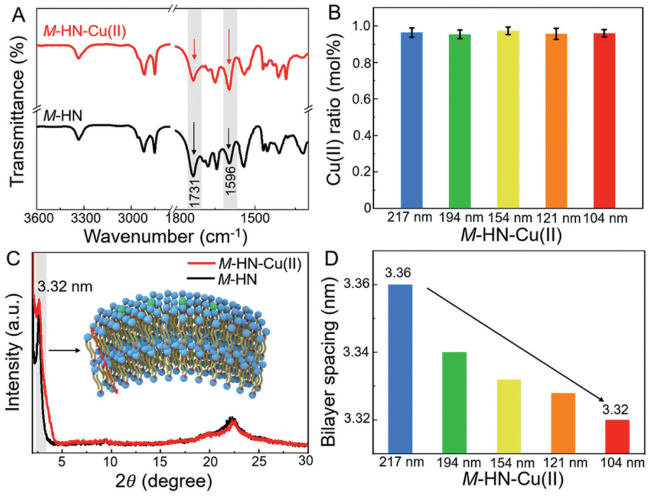

Fig. 2. (A) FTIR spectra of the *M*-HN–Cu(II) and *M*-HN with screw pitch of 104 nm. (B) ICP-AES determined Cu(II) ion loading on the five *M*-HN–Cu(II) samples. (C) XRD patterns of the *M*-HN–Cu(II) and *M*-HN with screw pitch of 104 nm. (D) Histogram of the bilayer spacing of the five *M*-HN–Cu(II) samples.

screw pitch length of 104 nm and largest tilt angle of 34° (Figs. 1G and H, Fig. S4 in Supporting information), demonstrating the most obvious extent of twist. The different helical twist level may be caused by the different extent of molecular interactions between the L-GluC$_{16}$ amphiphiles and each organic solvent, as proved by their -NH- peak shifts tested from the ^{1}H NMR spectra (Fig. S5 in Supporting information) [21,22]. Moreover, the *P*-HN–Cu(II) with the same screw pitch length and tilt angle can also be obtained from the self-assembly of D-GluC$_{16}$ amphiphiles (Figs. S6 and S7 in Supporting information) in the mixture of water and tetrahydrofuran (Fig. S8 in Supporting information).

To further confirm the Cu(II) ion loading onto *M*-HN, the Fourier transform infrared (FTIR) spectroscopy was obtained (Fig. 2A). The intensity of the vibration band for the carboxyl groups at 1731 and 1596 cm^{-1} is decreased and increased respectively upon the Cu(II) addition, suggesting the successful metal ion coordination between the carboxyl groups and Cu(II) [23,24]. The inductively coupled plasma atomic emission spectroscopy (ICP-AES) confirmed the added Cu(II) ions in solution were all successfully loaded on the five *M*-HNs with the similar loading amount of ~1 mol% (Fig. 2B). The X-ray diffraction (XRD) patterns of the *M*-HN–Cu(II) and *M*-HN with 104 nm pitch length are similar, indicating the metal coordination of Cu(II) had negligible influence on the arrangement of the molecular assembly (Fig. 2C). The sharp peak at 2.64° is assigned to the distance spacing of 3.32 nm, indicating the formation of a bilayer assembled structure [25,26]. With the increase of the screw pitch length from 104 nm to 217 nm, such bilayer distance spacing also expands from 3.32 nm to 3.36 nm (Fig. 2D and Fig. S9 in Supporting information), indicating the larger twist extent will aid to the tighter atomic distance and thus stronger molecular interactions [27].

We then investigated the dependence between the chiral morphology of different screw pitches and the enantioselectivity by catalyzing the D-A reaction of aza-chalcone and cyclopentadiene, since Cu(II) is a well-known catalyst to obtain the racemic products from the two reactants, and the endo products are energetically more favored over the exo products (Figs. S10-S12 and Table S1 in Supporting information) [28]. As shown in Table 1 (entries 1–5), all the five *M*-HN–Cu(II) samples have a high yield to produce the endo product. Moreover, the enantiomeric excess (*ee*) of the *S*-endo product determined by the chiral high performance liquid chromatography (HPLC) is increased from 11% to 50% with

Table 1
Diels-Alder reaction catalyzed by *M*/*P*-HN–Cu(II) and L-GluC$_{16}$-Cu(II)[a].

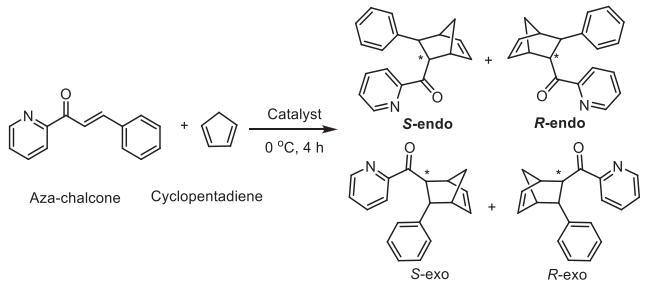

Entry	Catalyst	Yield (%)	endo:exo	*ee* (%, endo)
1	*M*-HN(217)-Cu(II)	94	98:2	11
2	*M*-HN(194)-Cu(II)	95	97:3	16
3	*M*-HN(154)-Cu(II)	94	98:2	23
4	*M*-HN(121)-Cu(II)	93	98:2	33
5	*M*-HN(104)-Cu(II)	95	98:2	50
6	*P*-HN(104)-Cu(II)	94	99:1	−50[b]
7	L-GluC$_{16}$-Cu(II)	36	98:2	0
8	L-GluC$_{16}$-Cu(II)	30	96:4	0
9	L-GluC$_{16}$-Cu(II)	22	99:1	0
10	L-GluC$_{16}$-Cu(II)	18	97:3	0
11	L-GluC$_{16}$-Cu(II)	0	NA	NA

[a] Reaction conditions: aza-chalcone (0.05 mmol), cyclopentadiene (0.5 mmol), catalysts (0.04 mmol), $Cu(NO_3)_2$ (1 mol%).
[b] -50 means the *ee* value of *R*-endo. The solvents used for entry 7–11 are acetone (10 mL), methanol (10 mL), ethanol (10 mL), acetonitrile (10 mL), tetrahydrofuran (10 mL), respectively.

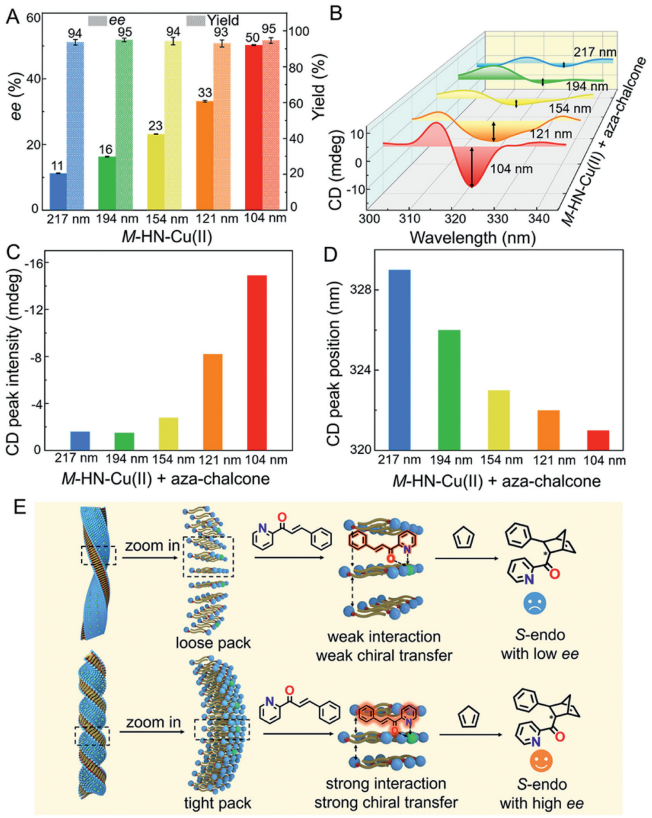

Fig. 3. (A) Histogram of the yield and *ee* value of the five *M*-HN–Cu(II) catalyzing the D-A reaction to obtain the *S*-endo product. (B) CD spectra of the aza-chalcone adsorbed on the five *M*-HN–Cu(II) samples. Histograms of the CD peak (C) intensity and (D) position of the aza-chalcone adsorbed on the five *M*-HN–Cu(II) samples. (E) Schematic illustration of the chiral transfer effect from the *M*-HN–Cu(II) with weak and strong twist to the aza-chalcone, leading to low and high *S*-endo product enantioselectivity, respectively.

the screw pitch reduced from 217 nm to 104 nm (Fig. S13, Table S2 in Supporting information). Such dramatic 4.5-fold increase of the *ee* value must originate from the chiral twist level of the assembled HNs, since the single L-GluC$_{16}$ amphiphiles with Cu(II) ions dissolved in each corresponding organic solvent did not demonstrate any enantioselectivity towards this reaction (Table 1, entries 7–11, Fig. S14 and Table S3 in Supporting information). The blank control experiments of D-A reaction catalyzed by Cu(II) ions alone show no catalytic enantioselectivity (0% *ee*, Fig. S15 and Table S4 in Supporting information), and the *M*-HN(121) host alone yield no catalytic reaction products at all (Table S4). These control experiments confirm that the formation of *M*-HN(121)-Cu(II) is the key to the increase of yield and *ee* value. Moreover, the dosage of catalyst mainly affects the yield of D-A reaction, less dosage leads to smaller yield, but has little effect on the catalytic enantioselectivity (Fig. S16, Tables S5 and S6 in Supporting information). Also, the *P*-HN–Cu(II) with 104 nm screw pitch length gave the similar yield and *ee* value of the *R*-endo product (Table 1, entry 6, Fig. S17 and Table S7 in Supporting information), displaying the chiral morphology-enantioselectivity dependence of our supramolecular catalysts in this asymmetric reaction.

To understand such chiral morphology-enantioselectivity relationship (Fig. 3A), we monitored the signal changes from both the FTIR and circular dichroic (CD) spectra for the samples of *M*-HN–Cu(II) with aza-chalcone adsorbed on their surfaces. First, from the FTIR spectra of the free aza-chalcone compared with the coupled *M*-HN–Cu(II)-aza-chalcone (Fig. S18 in Supporting information), the obvious peak shifts of the carbonyl groups vibration (1668–1674 cm^{-1}) and aromatic rings vibration (1601–1596 cm^{-1}) assigned for aza-chalcone demonstrated its successful adsorption on *M*-HN–Cu(II). Second, free aza-chalcone is an achiral molecule without CD signals. However, once aza-chalcone was adsorbed onto the *M*-HN–Cu(II) surface, the chiral transfer effect can occur from the *M*-HN–Cu(II) to aza-chalcone molecules, making the appearance of the negative (~325 nm) and positive (~315 nm) CD signal peaks assigned to aza-chalcone (Fig. 3B). It is noteworthy that since the *M*-HN–Cu(II) did not show CD signal peaks within that wavelength range [29], neither did the single mixture of L-GluC$_{16}$–Cu(II) monomers with aza-chalcones in the corresponding five organic solvents (Fig. S19 in Supporting information), such chiral transfer effect can only happen from the supramolecular assemblies to the aza-chalcones. As shown in Figs. 3B-D for the aza-chalcone adsorbed *M*-HN–Cu(II) samples with different screw pitch length, with the decrease of the screw pitch length from 217 nm to 104 nm, the intensity of the negative CD peaks of the adsorbed aza-chalcone increased from 1.5 mdeg to 14.9 mdeg and the peak position also shifted from 329 nm to 321 nm, indicating the stronger chiral transfer effect and weaker π-π interaction between the aza-chalcone molecules. Moreover, the larger binding constant K_a (obtained from the ultraviolet-titration, Fig. S20 in Supporting information) between the aza-chalcone and *M*-HN–Cu(II) was measured for the smaller screw pitch length, further confirming the stronger interactions exist between the more twisted *M*-HN–Cu(II) and the reactants.

From all the experimental results above-mentioned, the morphology-enantioselectivity relationship in our system can be understood as follows (Fig. 3E): the water/organic solvent regulated self-assembly of L-GluC$_{16}$ amphiphiles and Cu(II) ions give a series of *M*-HN–Cu(II) samples with different twist extent, with the smaller screw pitch one having tighter atomic distance and stronger monomeric intermolecular interactions. During the D-A reaction, the aza-chalcone as reactant can bind to Cu(II) as catalytic center through the coordination of O and N atoms [17]. Meanwhile,

the aza-chalcone can also be influenced by the amphiphile units, and the interaction between them is stronger with the tighter atomic arrangement of the amphiphiles, which is reflected by the more obvious chiral transfer effect. Thus, when the second reactant of cyclopentadiene was added, the reaction can demonstrate different enantioselectivity with the ones having different screw pitches.

In conclusion, a series of supramolecular *M*/*P*-HNs assembled from the chiral L/D-GluC_{16} amphiphiles and Cu(II) ions were facilely obtained, with their helical screw pitches adjusted from 217 nm to 104 nm through the regulation of their water/organic solvent assembly environment. They were then used as ideal models to investigate the chiral morphology-enantioselectivity dependent relationship by catalyzing the asymmetric D-A reaction to obtain the endo-product with different *ee* values. Experimental results reveal the chiral supramolecular HNs with more twisted extent (smaller screw pitch length and larger tilt angle) tend to have higher enantioselectivity during the D-A reaction, which is caused by the stronger interactions between the reactants and the supramolecular HNs, leading to the stronger chiral transfer effect. Our study provides a new aspect to rationally control the supramolecular assemblies as catalysts and supplies guidance for designing chiral supramolecular catalysts with higher enantioselectivity.

Declaration of competing interests

The authors declare that they have no known competing financial interests or personal relationships that could have appeared to influence the work reported in this paper.

CRediT authorship contribution statement

Cong Gao: Writing – original draft, Formal analysis, Data curation. **Zijian Zhu:** Writing – original draft, Data curation. **Siwei Li:** Data curation. **Zheng Xi:** Writing – review & editing, Supervision, Formal analysis. **Qingqing Sun:** Writing – review & editing. **Jie Han:** Writing – review & editing, Validation, Supervision, Funding acquisition, Conceptualization. **Rong Guo:** Writing – review & editing.

Acknowledgments

The authors gratefully acknowledge the support of this research by the National Natural Science Foundation of China (Nos. 22202171, 21922202, and 22272146), the Natural Science Foundation of Jiangsu Basic Research Program (No. BK20220559), the Natural Science Foundation of the Higher Education Institutions of Jiangsu Province (No. 22KJD150009), and the Jiangsu Specially-Appointed Professor Plan (Z. Xi) from the Jiangsu Education Department.

Supplementary materials

Supplementary material associated with this article can be found, in the online version, at doi:10.1016/j.cclet.2024.109968.

References

[1] M. Liu, L. Zhang, T. Wang, Chem. Rev. 115 (2015) 7304–7397.
[2] J. Dong, Y. Liu, Y. Cui, Acc. Chem. Res. 54 (2021) 194–206.
[3] Y. Sang, M. Liu, Chem. Sci. 13 (2022) 633–656.
[4] J. Li, Y. Tang, Q. Wang, et al., J. Am. Chem. Soc. 134 (2012) 18522–18525.
[5] L. Xu, L. Zhou, Y.X. Li, et al., Nat. Commun. 14 (2023) 7287.
[6] C. Wang, G. Yuan, C. Wang, et al., Small Struct. 4 (2023) 2200405.
[7] G. Yuan, Z. Xi, C. Wang, et al., Acta Phys. Chim. Sin. 39 (2023) 2212061.
[8] W. Xuan, M. Zhang, Y. Liu, Z. Chen, Y. Cui, J. Am. Chem. Soc. 134 (2012) 6904–6907.
[9] C.G. Claessens, T. Torres, J. Am. Chem. Soc. 124 (2002) 14522–14523.
[10] Y. Sun, Y. Meng, J. Jiang, H. Sun, T. Li, Chin. Chem. Lett. 30 (2019) 966–968.
[11] K. Chen, Z. He, W. Xiong, C.J. Wang, X. Zhou, Chin. Chem. Lett. 32 (2021) 1701–1704.
[12] Z. Wu, H. Qian, X. Li, T. Xiao, L. Wang, Chin. Chem. Lett. 35 (2024) 108829.
[13] A. Desmarchelier, X. Caumes, M. Raynal, et al., J. Am. Chem. Soc. 138 (2016) 4908–4916.
[14] S. Wang, H. Jiang, L. Zhang, J. Jiang, M. Liu, ChemPlusChem 83 (2018) 1038–1043.
[15] Z. Shen, Y. Sang, T. Wang, et al., Nat. Commun. 10 (2019) 3976.
[16] K.S. Lee, J.R. Parquette, Chem. Commun. 51 (2015) 15653–15656.
[17] J. Jiang, Y. Meng, L. Zhang, M. Liu, J. Am. Chem. Soc. 138 (2016) 15629–15635.
[18] F. Rodríguez-Llansola, J.F. Miravet, B. Escuder, Chem. Commun. (2009) 7303–7305.
[19] S. Bhowmick, L. Zhang, G. Ouyang, M. Liu, ACS Omega 3 (2018) 8329–8336.
[20] X. Wu, M. Liu, C. Zheng, et al., Chin. Chem. Lett. 34 (2023) 107590.
[21] F. Wang, M. Qin, T. Peng, et al., Langmuir 34 (2018) 7869–7876.
[22] J.G. Jia, C.C. Zhao, Y.F. Wei, et al., J. Am. Chem. Soc. 145 (2023) 23948–23962.
[23] Q. Jin, L. Zhang, H. Cao, et al., Langmuir 27 (2011) 13847–13853.
[24] F. Wang, C. Feng, Angew. Chem. Int. Ed. 130 (2018) 5757–5761.
[25] X. Zha, Y. Chen, H. Fan, et al., Angew. Chem. Int. Ed. 60 (2021) 7759–7769.
[26] G. Das, R. Thirumalai, B. Vedhanarayanan, V.K. Praveen, A. Ajayaghosh, Adv. Opt. Mater. 8 (2020) 2000173.
[27] Q. Jin, L. Zhang, X. Zhu, P. Duan, M. Liu, Chem. Eur. J. 18 (2012) 4916–4922.
[28] D.X. Zhao, Z.Z. Xu, Z.Z. Yang, Chin. Chem. Lett. 19 (2008) 1135–1138.
[29] C. Gao, S. Li, C. Zhao, et al., Small 20 (2024) 2310234.